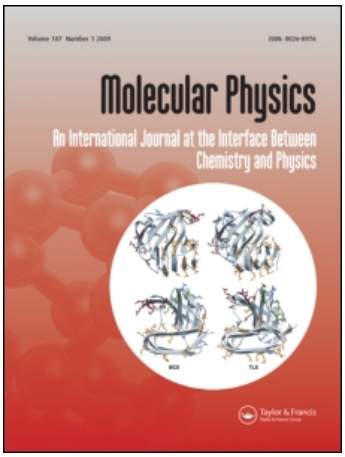

Molecular Physics
Publication details, including instructions for authors and subscription information:
http://www.informaworld.com/smpp/title~content=t713395160

Molecular dynamics investigations of the electrostatic interactions in liquid carbonyl sulphide

H. Stassen [a]; Th. Dorfmüller [a]; J. Samios [b]
[a] Fakultät für Chemie, Physikalische Chemie I, Universität Bielefeld, Bielefeld 1, Germany [b] Department of Chemistry, Physical-Theoretical Chemistry, University of Athens, Athens, Greece

Online Publication Date: 10 October 1992

To cite this Article Stassen, H., Dorfmüller, Th. and Samios, J.(1992)'Molecular dynamics investigations of the electrostatic interactions in liquid carbonyl sulphide',Molecular Physics,77:2,339 — 350
To link to this Article: DOI: 10.1080/00268979200102481
URL: http://dx.doi.org/10.1080/00268979200102481

MOLECULAR PHYSICS, 1992, VOL. 77, NO. 2, 339–350

Molecular dynamics investigations of the electrostatic interactions in liquid carbonyl sulphide

By H. STASSEN, TH. DORFMÜLLER
Fakultät für Chemie, Physikalische Chemie I, Universität Bielefeld, D-4800 Bielefeld 1, Germany

and J. SAMIOS
Department of Chemistry, Physical-Theoretical Chemistry, University of Athens, Athens, Greece

(*Received 20 December 1991; accepted 27 February 1992*)

Molecular dynamics simulation was used to obtain information concerning the electrostatic contributions of dipole, quadrupole and octupole moments to the pair potential of liquid carbonyl sulphide. The influence of electrostatics is determined by the equilibrium properties of the liquid. These indicate that taking into account dipole and quadrupole moments, results are obtained in accordance with the Lennard-Jones model. Potential models including the octupole moment are shown to give a less adequate description of the liquid carbonyl sulphide.

1. Introduction

In molecular dynamics (MD) simulation of liquids, a central problem that arises is the description of intermolecular interactions with pairwise additive potential models. Since multibody interactions are not taken explicitly into account by these pair potentials, the effective and empirical character of such interaction models becomes evident. A more detailed picture of the intermolecular interaction requires the separation of the potential model into several distinct terms each having a theoretical basis, such as electrostatic potentials, dispersion energies, induction interactions, overlap effects, and so on. The explicit introduction of these contributions in MD simulations, however, entails great expense of computer processing (CPU) time and is not realizable in systems consisting of several hundreds of molecules, which are necessary to achieve accurate statistics.

On the other hand, the interaction model used in an MD simulation is of course expected to reproduce the experimental picture of the investigated liquid as accurately as possible. This is the most reliable test against artefacts in the dynamical analysis of calculated trajectories. This becomes very important in the case of the computation of collision-induced phenomena, because additional approximations such as induction models have to be used. Thus, for MD simulations of liquids the best compromise between the accuracy of the results and the simplicity of the pair potential has to be found in each particular case.

In the case of the polar liquid carbonyl sulphide (OCS), it seems to be obvious that electrostatic moments of the molecules have to be taken into account by the interaction model. In a previous MD investigation [1] it has been shown that the equilibrium properties of the liquid OCS in the temperature range 243–300 K may be satisfactorily described by an interaction model consisting only of a site–site 12-6

0026-8976/92 $3.00

Lennard-Jones (LJ) potential model. Including the small molecular dipole μ, the quadrupole Q, as well as the large octupole Ω ($\mu = 0{\cdot}72\,\mathrm{D}$, $Q = -0{\cdot}79\,\mathrm{D\AA}$, and $\Omega > 10\,\mathrm{D\AA}^2$ [2]), a model study is presented of the influence of electrostatic multipoles on the thermodynamic properties and structural features of liquid OCS. It is assumed that all other types of interaction can be incorporated in the anisotropic LJ potential. The point molecular multipole model of electrostatic interactions is used, since the introduction of point charges, representing the molecular multipoles, or atomic multipole moments, produces additional uncertainties about the magnitude and localization of these properties.

The present work may therefore be regarded as an extension of the first investigation [1] with the aim to compare a number of effective molecular pair potential models for liquid OCS. The paper is organized as follows. In section 2 the interaction model of two charge distributions according to multipole expansion theory [3] is reviewed. A presentation of the potential models used in the MD simulations is given in section 3 together with some computational details. In sections 4 and 5 the simulated thermodynamic results and structural pair distribution functions are reported and discussed. A short summary of the main findings concludes this article in section 6.

2. Electrostatic interactions

Using the Cartesian tensor formalism, the interaction energy between two multipoles of order l and m is given by

$$v^{lm} = \frac{(-)^l}{(2l-1)!!(2m-1)!!} \boldsymbol{M}^{(l)} \cdot \boldsymbol{T}^{(l+m)} \cdot \boldsymbol{M}^{(m)} \tag{1}$$

where $\cdot$ indicates a full contraction of two tensors and the term $(2l-1)!!$ is defined as $(2l-1)(2l-3)\ldots(5)(3)(1)$. The tensor $\boldsymbol{T}^{(l)}$ contains the distance-dependent contribution to v and is built by the lth derivation of the reciprocal distance vector $\mathbf{r}_{ij}$ between the centres of mass of molecules i and j with respect to the component for each direction

$$\boldsymbol{T}^{(l)}(\boldsymbol{r}_{ij}) = \nabla^l \frac{1}{\boldsymbol{r}_{ij}} \tag{2}$$

The orientation-dependent multipole tensors $\boldsymbol{M}^{(l)}$ correspond to the charge $q(l=0)$, dipole $\mu(l=1)$, quadrupole $Q(l=2)$, octupole $\Omega(l=3)$, and higher moments. For the axially symmetric charge distribution of a linear molecule, the components of these tensors may be obtained from the permanent multipole $\boldsymbol{M}_0^{(l)}$ and the unit vector $\hat{\boldsymbol{u}}$ of the molecular axis in the frame of the system, inserted into the corresponding Legendre polynomial

$$\mu_\alpha = \mu_0 \cdot u_\alpha \tag{3}$$

$$Q_{\alpha\beta} = Q_0 \cdot \tfrac{1}{2}(3u_\alpha u_\beta - \delta_{\alpha\beta}) \tag{4}$$

$$\Omega_{\alpha\beta\gamma} = \Omega_0 \cdot \tfrac{1}{2}(5u_\alpha u_\beta u_\gamma - u_\gamma\delta_{\alpha\beta} - u_\beta\delta_{\alpha\gamma} - u_\alpha\delta_{\beta\gamma}) \tag{5}$$

where the greek indices denote the x-, y-, or z-direction, respectively; and δ is the Kronecker δ-function.

Regarding the dipole as the lowest and the octupole as the highest electrostatic moment of the OCS molecule ($C_{\infty v}$-symmetry), the total interaction energy v_{ij} between

a pair of molecules i and j is a sum over all combinations of multipole interactions v^{lm} from equation (1)

$$v_{ij} = \sum_{l=1}^{3} (-)^l \sum_{m=1}^{3} \frac{\boldsymbol{M}^{(l)} \cdot \boldsymbol{T}^{(l+m)} \cdot \boldsymbol{M}^{(m)}}{(2l-1)!!(2m-1)!!}. \tag{6}$$

The forces $\boldsymbol{f}_{ij}$, defined by $\boldsymbol{f}_{ij} = -\nabla v_{ij}$, are easily obtained from equation (6) using the tensor $\boldsymbol{T}^{(l+m+1)}$ multiplied by -1. A change of sign in $\boldsymbol{f}_{ij}$ leads to the forces $\boldsymbol{f}_{ji}$. The definition of the torques, $\boldsymbol{t}_{ij} = -\hat{\boldsymbol{u}}_i \times \nabla_{\hat{\boldsymbol{u}}_i} v_{ij}$, where $\nabla_{\hat{\boldsymbol{u}}_i}$ indicates a derivation with respect to the components of $\hat{\boldsymbol{u}}_i$, may be simplified, since only the multipole tensors in equation (6) are dependent on $\hat{\boldsymbol{u}}_i$, but a change of sign in order to compute the $\boldsymbol{t}_{ji}$ is prevented. Consequently, the $\boldsymbol{t}_{ji}$ have to be evaluated explicitly.

The full tensor contraction in equation (6) enables the introduction of scalar products of the type

$$\cos\gamma = \hat{\boldsymbol{u}}_i \cdot \hat{\boldsymbol{u}}_j \tag{7}$$

$$\cos\theta_i = \frac{\hat{\boldsymbol{u}}_i \cdot \boldsymbol{r}_{ij}}{r_{ij}} \tag{8}$$

$$\cos\theta_j = \frac{\hat{\boldsymbol{u}}_j \cdot \boldsymbol{r}_{ij}}{r_{ij}} \tag{9}$$

and the terms of the sums in equation (6) are reduced to simple relations [4]. Making use of this technique, the dipole–dipole interaction energy is for example given by

$$v_{ij}^{\mu\mu} = \frac{\mu^2}{r_{ij}^3} (\cos\gamma - 3\cos\theta_i \cos\theta_j) \tag{10}$$

The application of equations (7–9) results in an important economy in processing time.

3. Computational details

In this study, various electrostatic interactions from equation (6) have been combined with the previously reported site–site LJ potential [1]. The applied potential models are (l denotes the multipole moments used according to equation (6); $l = 1$: dipole, $l = 2$: quadrupole, $l = 3$: octupole):

Model A: LJ without electrostatics
Model B: LJ + v^{ll}; $l = 1$
Model C: LJ + v^{ll}; $l = 1, 2$
Model D: LJ + v^{ll}; $l = 3$
Model E: LJ + v^{ll}; $l = 1, 2, 3$

Since the molecular quadrupole moment of OCS is found to be smaller than those of other linear axially symmetric molecules [5] and superposed by the dipole of the molecule, a potential model containing site–site LJ and only quadrupole–quadrupole interactions for the electrostatic part is believed to be inadequate. The potential parameters used in the simulations are tabulated in table 1.

NVE-MD simulations were performed with 864 OCS molecules in a cubic box with the usual periodic boundary conditions. A spherical cutoff radius was taken at 0·35 of the box length. At this distance the electrostatic contribution is less than 3% of the internal energy arising from purely LJ interaction and, thus, a long-range

Table 1. Site–site LJ potential parameters and molecular multipole moments [2] of OCS. The cross LJ interaction parameters are obtained using the Lorentz–Berthelot mixing rule.

LJ parameter	S–S	C–C	O–O
ε[K]	178·0	29·0	78·0
σ[nm]	0·360	0·284	0·302
Multipoles	$\mu = 0{\cdot}72\,\mathrm{D}$	$Q = -0{\cdot}79\,\mathrm{D\AA}$	$\Omega = 10\,\mathrm{D\AA}^2$

correction for potential energy and virial function only is taken on the LJ potential model. The translational and rotational equations of motions were solved using a fifth and a fourth order Gear predictor–corrector algorithm, respectively. The integration time-step Δt was $3{\cdot}5 \times 10^{-15}$ s. Starting with the molecules arranged on an f.c.c. lattice structure, equilibrium was achieved after 10 000 time steps. The MD trajectories were extended to 60 ps. All MD runs were carried out on a Convex C240 four-processor computer using the O2 compiler option for vectorization.

The potential models were tested at the thermodynamic state ($T = 300\,\mathrm{K}$, $V_M = 62{\cdot}14\,\mathrm{cm^3\,mol^{-1}}$ [6]), where the internal energy for the liquid predicted by model A shows the best agreement with experimental results. Bond lengths d_{CS} and d_{CO} were taken from gas-phase experimental results to be equal to 1·561 Å and 1·164 Å [7, 8], respectively.

4. Thermodynamic results

For each potential model the obtained configurational energies U and pressures P are compared with experimental results in table 2. Satisfactory agreement between simulation and experiment is found for the potential models A, B, and C. Since differences in the results obtained from these models are negligible, it is suggested that the small dipole and quadrupole moments do not affect the equilibrium properties of liquid OCS. The potential models including octupole–octupole interactions yield energies and pressures that are too negative. The LJ contribution to U for models D and E amounts to $-12{\cdot}5$ and $-12{\cdot}6\,\mathrm{kJ\,mol^{-1}}$, respectively, and is in accordance with the result of model A. Thus, the additional attraction in the liquid OCS described by models D and E of 1·7 and 0·8 kJ mol^{-1} is due to the direct effect of octupole–octupole interaction and not to a modification of the LJ potential by electrostatic interactions. This behaviour indicates that the octupole–octupole interaction seems to be well taken care of by the LJ site–site model.

In the case of model E the pure octupole–octupole energy amounts to

Table 2. Thermodynamic results for the various potential models.

Model	U/kJ mol^{-1}	P/bar	$\langle F^2\rangle/10^{-20}\,\mathrm{N^2}$	$\langle T^2\rangle/10^{-39}\,\mathrm{J^2}$	$D/10^{-5}\,\mathrm{cm^2\,s^{-1}}$
A	−12·7	32	9·46	1·17	5·17
B	−12·8	5	9·45	1·17	5·28
C	−12·8	4	9·49	1·18	5·18
D	−14·2	−670	11·24	1·71	5·40
E	−13·4	−370	10·54	1·48	4·83
Experimental	−12·5[a]	12·8	–	–	–

[a] Calculated from the heat of vapourization by $U = RT - \Delta H_{vap}$.

$-1\,\mathrm{kJ\,mol^{-1}}$, which is $0{\cdot}7\,\mathrm{kJ\,mol^{-1}}$ less attractive than in model D due to the influence of other electrostatic moments. Some contributions to U arising from the combination of different moments, especially from the dipole–octupole interaction, have repulsive character in the liquid described by model E.

Table 2 contains also the mean-squared forces $\langle F^2 \rangle$ and torques $\langle T^2 \rangle$, computed as a time and ensemble average of the forces and torques, and the diffusion coefficients D, calculated for each potential model from the mean-squared displacements of the molecules

$$\lim_{t\to\infty} \frac{\partial}{\partial t} \langle (\boldsymbol{R}_i(t) - \boldsymbol{R}_i(0))^2 \rangle = 6D, \tag{11}$$

where $\boldsymbol{R}_i$ is the position of molecule i. The results illustrate the excellent agreement between models A, B, and C, whereas models D and E produce values differing significantly from these. Thus, the octupole–octupole interaction exhibits a similar influence on these properties as discussed in the case of the internal energy.

The calculated $\langle F^2 \rangle$ and $\langle T^2 \rangle$ of models A, B, and C may be compared with the corresponding results of MD simulations on liquid CO_2 [9] and CS_2 [10]. Assuming only a weak temperature dependence of these properties, $\langle F^2 \rangle$ and $\langle T^2 \rangle$ of liquid OCS are found to be of the order of magnitude of CO_2, but distinctly smaller than in CS_2.

The diffusion coefficient of liquid OCS exceeds an experimental value of $D = 4{\cdot}2 \times 10^{-5}\,\mathrm{cm^2\,s^{-1}}$ for CS_2 at 294 K [10] by approximately 25%. Simulated diffusion coefficients of CO_2 computed from the velocity autocorrelation functions at temperatures below 250 K at various densities [11] exceed the OCS results given here, and it is concluded that OCS takes an intermediate position between CO_2 and CS_2 concerning the diffusion coefficients.

5. Pair correlation functions

With the aim of comparing the structural directing effects of the different potential models, the centre-of-mass (COM) and the six independent atom–atom radial pair correlation functions $G(r)$ were computed for the liquid OCS. These functions are defined by the number of molecules or atoms whose distance lies in a certain interval, normalized to the ideal gas density of the corresponding thermodynamic state as a function of distance

$$G(r) = \frac{1}{4\pi N \rho r^2} \left\langle \sum_{i=1}^{N} \sum_{j\neq 1}^{N} \delta(r - r_{ij}) \right\rangle. \tag{12}$$

The various possible orientations of the molecules are indirectly included in the complete set of atom–atom pair correlation functions.

Peak positions and heights of the first two maxima and the first minimum in the COM pair correlation functions G_{MM} are presented in table 3. The functions are illustrated in figure 1 up to a distance of 1 nm. It is obvious that the dipole (model B) and quadrupole (model C) moments of OCS do not influence the G_{MM} of the LJ model A, but inclusion of the large molecular octupole changes G_{MM} dramatically. Model D broadens the first peak and yields a strong short-range shoulder at 0·39 nm, which is also found in the G_{MM} of liquid CS_2 [12]. A tendency to form a weak shoulder at the first peak is observed in the G_{MM} of the other potential models and is increased at lower temperatures [1]. Model E results in a G_{MM} which may be characterized as the average of the functions from models A and D.

Table 3. Positions and peak heights of the first two maxima and the first minimum of the centre-of-mass pair correlation functions obtained by the different potential models.

	First maximum		First minimum		Second maximum	
Potential model	r/nm	$G(r)$	r/nm	$G(r)$	r/nm	$G(r)$
A	0·47	1·42	0·67	0·87	0·84	1·04
B	0·47	1·42	0·66	0·87	0·83	1·05
C	0·47	1·43	0·65	0·87	0·84	1·05
D	0·47[a]	1·31	0·65	0·91	0·81	1·04
E	0·47[a]	1·38	0·66	0·89	0·85	1·04

[a]Shoulder at 0·39 nm with $G(r) = 1·02$.

The first shell coordination numbers are 11·8 for the potential model A, B, and C, 10·7 for model D, and 11·0 in the case of model E. Thus, results for G_{MM} indicate a similar dependence on the potential model as the computed thermodynamic properties of section 4.

The effect of the potential models used on the centre-of-mass pair correlation functions and thermodynamic properties show that octupole–octupole interactions change the results of liquid OCS predicted by an LJ model significantly. Differences between models D and E are due to cross interactions of the large octupole moment with the smaller dipole and quadrupole moments. Thus, it is suggested that the consideration of octupole–octupole interaction as the only electrostatic term may not be able to describe OCS in the liquid state, and no further discussion of model D is attempted.

Unfortunately, information on structural features of the liquid OCS from x-ray and neutron scattering experiments is not available in the literature. Therefore, at this stage no more definite answer to this problem can be given, and discussion is limited to a comparison of the atom–atom pair correlation functions G_{AB} (A, B = C, O, S) obtained by the different potential models A, B, C, and E. These functions are presented in figures 2–7.

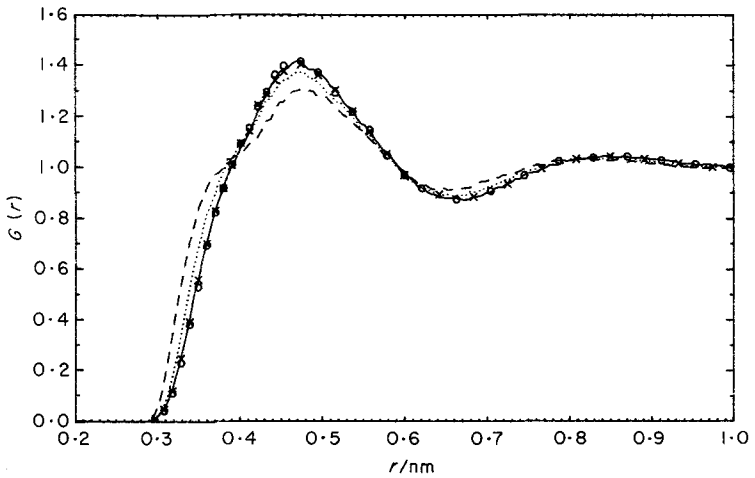

Figure 1. Centre-of-mass pair correlation functions for the five potential models: solid line, model A; crosses, model B, circles, model C; dashed line, model D; dotted line, model E.

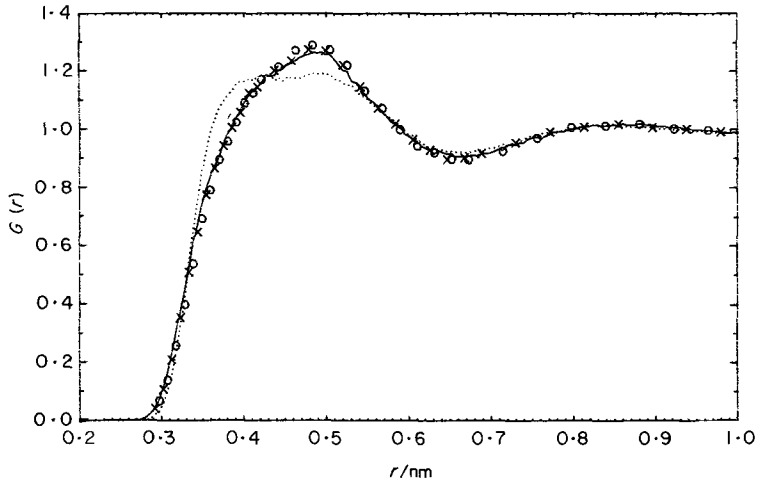

Figure 2. CC pair correlation functions for the potential models: solid line, model A; crosses, model B, circles, model C; dotted line, model E.

The G_{CC} in figure 2 are characterized by very broad extrema. The functions of models A, B, and C show a first maximum at 0·49 nm followed by a minimum at 0·67 nm. A very small shift to larger distances is found going over from model A to C. Also, the first peak height increases when the dipole and quadrupole interactions are considered (model A: 1·25, model B: 1·27, model C: 1·30). The unbalanced shape of the first peak of these models indicates local structures between 0·35 and 0·45 nm, which are very strongly pronounced by model E. A broad plateau is found between 0·39 and 0·51 nm as the first maximum peak.

In figure 3 the G_{CS} are presented. The models A, B, and C show a symmetric first peak at 0·43 nm with a height of 1·28. In contrast to the G_{CC} of these models, a small shift to shorter distances due to dipole and quadrupole interaction is observed. The occurrence of two maxima in the first peak as in liquid CS_2 [12] is not found for these

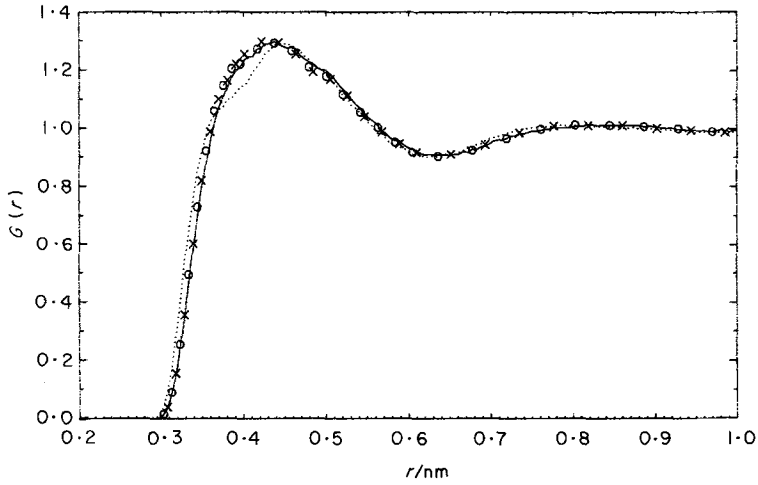

Figure 3. CS pair correlation functions for the potential models: solid line, model A; crosses, model B; circles, model C; dotted line, model E.

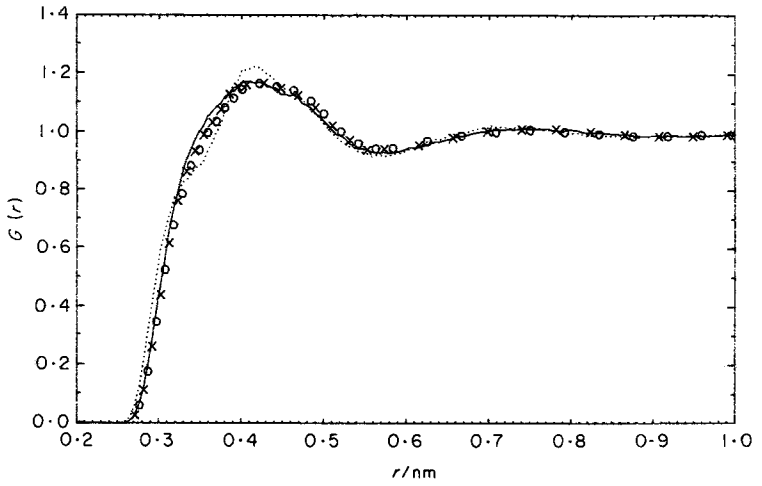

Figure 4. CO pair correlation functions for the potential models: solid line, model A; crosses, model B; circles, model C; dotted line, model E.

models, but is indicated by the strong shoulder at 0·37 nm for model E. Thus, introduction of the octupole–octupole interaction changes the LJ G_{CS} in a direction corresponding to this function for CS_2.

The shapes of the G_{CO} of models A, B, and C from figure 4 comply with the corresponding G_{CS}. As a consequence of the shorter bond length d_{CO} the extrema of the G_{CO} appear at smaller distances (first maxima at 0·42 nm), but more broadened, than in the G_{CS} of these models. In opposition to the dipole- and quadrupole-influenced G_{CS}, a small shift to larger distances than in the LJ model A of the G_{CO} modelled by potentials B and C is observed. Since the COM of OCS is localized on the C–S bond, this shift agrees with findings in the G_{CC} of OCS. The additional octupole–octupole interaction determines a shoulder in front of the first peak at 0·34 nm, which is less distinct than in the corresponding G_{CS}, followed by a maximum at 0·4 nm. In contrast to G_{CC} and G_{CS} the first peak in G_{CO} of model E is diminished in comparison with the results for model A.

The G_{SS} of figure 5 are similar for all potential models. A sharp first maximum at 0·39 nm is followed by a minimum at 0·54 nm and a weak maximum at 0·59 nm. The shape of these functions differs significantly from the CS_2 G_{SS} [12]. Peak heights of the first maximum present a potential dependence. The lowest peak (1·60) is found for the potential model B, the consideration of the quadrupole yields a height of 1·62. The G_{SS} of these models are less intensive than the LJ result with a first maximum height of 1·66. Model E raises the first peak to 1·72 and decreases the first minimum by 0·03 compared with model A.

Figure 6 contains the G_{SO} of the simulations. All the functions are shaped like the high temperature G_{SS} of CS_2 [12]. The LJ model and the potentials including dipole and quadrupole moments exhibit a sharp maximum at 0·36 nm and a broad minimum in the region of 0·5 nm. Models B and C are nearly identical and surpass the G_{SO} of model A in the first peak height. The G_{SO} of the octupole containing model E is shifted by 0·01 nm to smaller distances and is more intense in peak height.

The situation becomes more complicated in the G_{OO} from figure 7. The result of model A is shaped similarly to the atom–atom pair correlation function of a two-

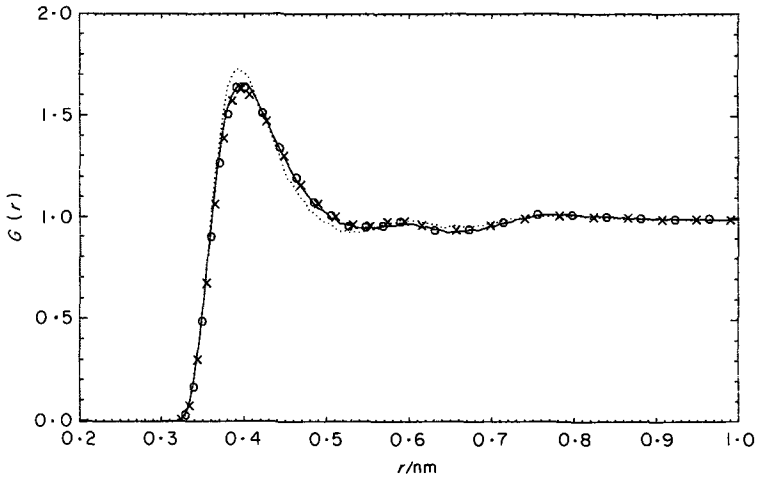

Figure 5. SS pair correlation functions for the potential models: solid line, model A; crosses, model B; circles, model C; dotted line, model E.

centre LJ model of CO_2 [9] with the exception of the small maximum which is found for CO_2 in the region behind the first minimum. In OCS the LJ first maximum appears at 0·33 nm with a peak height of 1·31. The second maximum at 0·61 nm is sharper than in the pair correlation functions of the other atoms. Models B and C produce a G_{OO} with small peak heights in the first (1·21) and higher peaks in the second maximum compared with model A. The decrease of G_{OO} between the first maximum and minimum of model C is more abrupt than in model B. In the G_{OO} of model E the first maximum with height 1·40 surpasses the G_{OO} of all potential models. The decay into the minimum is very precipitous. The second maximum of model E is dominated by the influence of dipole and quadrupole electrostatics, since G_{OO} of models B, C, and E coincide in this range.

Model E contains the complete electrostatic interaction potentials up to the

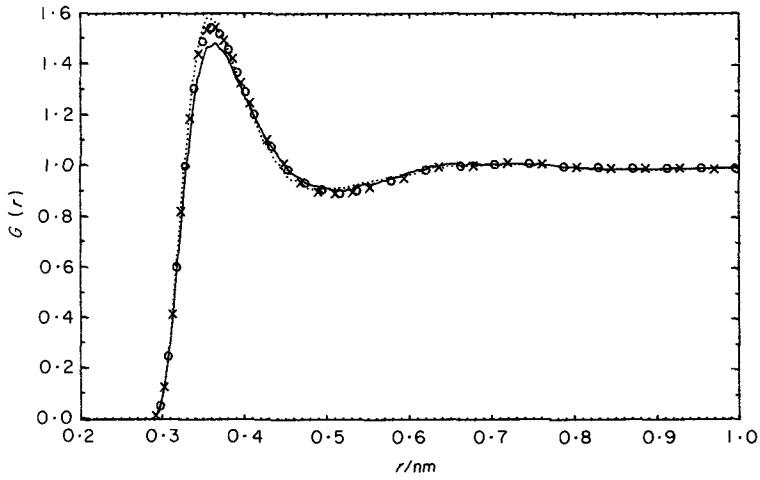

Figure 6. SO pair correlation functions for the potential models: solid line, model A; crosses, model B; circles, model C; dotted line, model E.

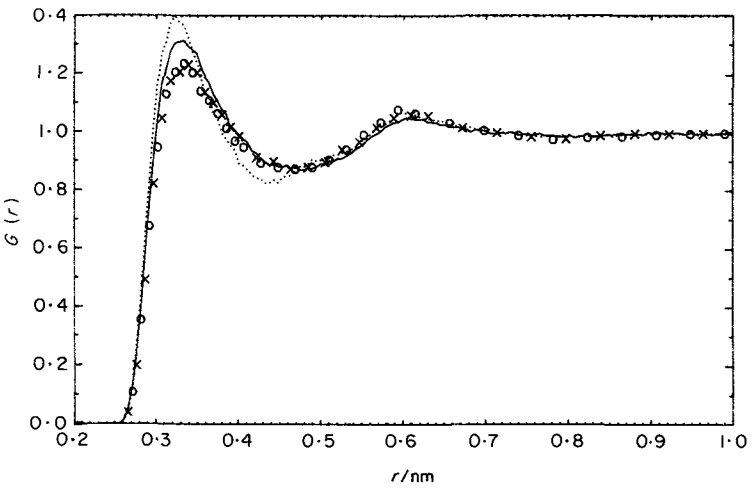

Figure 7. OO pair correlation functions for the potential models: solid line, model A; crosses, model B; circles, model C; dotted line, model E.

octupole. All G_{AB} for this model indicate the influence of the large octupole moment. A difference between models A and B occurs in the peak heights of G_{SS}, G_{SO}, and G_{OO}. When the dipole is taken into account, G_{OO} and G_{SS} decrease, while G_{SO} shows a remarkable increase in the height of the first peak. Since G_{CO}, G_{CS}, and G_{CC} are only very weakly affected, a small change in the orientation of two neighbour molecules due to dipolar interactions is assigned to this. All the G_{AB} of model C are in accordance with model B. Thus, the quadrupole interactions have only a small influence on the structural picture of the dipole–dipole electrostatics.

6. Conclusions

On the basis of the three-centre LJ model, which was previously developed in order to describe the equilibrium properties of liquid OCS, the influence of electrostatic interactions on thermodynamic properties and liquid structure has been investigated. In addition to the LJ model, four types of electrostatic interactions applying the one-centre multipole expansion theory have been tested.

Results indicate that the inclusion of dipole and quadrupole interactions agree with the LJ model for thermodynamic properties, mean-squared forces and torques, as well for diffusion coefficients. A small change in the orientation of molecules in the first shell is found for these models when higher order multipoles are included. It is suggested that the potential models A, B, and C give a realistic picture of liquid OCS as far as the observed properties in this study are concerned.

Approximating the electrostatic interaction of OCS with an octupole–octupole potential, negative internal energies and pressures are found to be too high. This result might be expected since additional terms have been added to a potential function which reproduces the experimental data. Note that a variation of the LJ parameter might of course correct for the differences between simulation and experiment. Such a procedure might lead to smaller values for the LJ parameters of OCS in order to adjust the internal energy, but it is questionable whether the corrected ε- and σ-values reproduce the shape of the molecule consistent with CO_2 and CS_2. On the other hand, it may be seen from the results for model E, which takes all the multipoles up to the

internal moment into account, that remarkable contributions to the internal energy arise from cross interactions between different kinds of multipoles. This indicates that model D with electrostatic interactions containing only octupole–octupole terms is not a conceivable description of liquid OCS, as far as thermodynamic properties are concerned.

The internal energy of model E indicates that a small variation of the LJ parameters may produce agreement with experiment. Since the magnitude of the molecular octupole moment of OCS is not accurately known, calculations were performed using a value of 10 DÅ^2, which is smaller than the proposed 12–15 DÅ^2 of Deakin and Walmsley [2]. Thus, a modified set of LJ parameters combined with an octupole moment of 12–15 DÅ^2, which could bring the internal energy of the simulation into agreement with experiment, could probably not represent the shape of the OCS molecule.

The intermolecular structure of liquid OCS predicted by model E indicates a strong influence of the octupole moment. Thus, the atom–atom pair correlation functions for this model differ significantly from the models A, B, and C. The G_{CC}, G_{CO}, and G_{CS} of model E exhibit first maximum peaks which have a different shape from the corresponding functions of the non-octupole containing models. Model E produces short-range local structures more than the other models and, since these differences are less marked in G_{OO}, G_{SO}, and G_{SS}, this finding may be a consequence of the point multipole expansion used in these simulations. The multipoles were placed on the COMs of the molecules and, due to the attractive octupole–octupole interaction, artificial isotropies were introduced to the potential function, which becomes obvious at short distances, even in that region where an anisotropic treatment of intermolecular interaction is most important. At distances beyond the first maximum of the pair correlation functions the influence of electrostatic interactions decreases. Thus, some indications for a weakness of the conventional multipole expansion in the description of short-range interactions may have been found in the simulations presented here.

These considerations suggest the application of a distributed multipole expansion [14] in the case of liquid OCS. Due to the introduction of additional interaction centres on each molecule, such a procedure may prevent the loss of anisotropic interaction at short distances. On the other hand, the implementation of a distributed multipole expansion into an MD simulation leads to greatly increased CPU time, even if the long-range interaction is described by conventional multipoles.

In conclusion, the three potential models A, B, and C are found to give a realistic description of the equilibrium properties of OCS. Since experimental information about the liquid structure is not available, it cannot be deduced from this study whether it is important to consider dipole and quadrupole moments in a potential model for the liquid OCS. The investigation of dynamical properties of the fluid may offer an answer to this question. In a forthcoming paper the authors deal with such data.

The authors Samios and Dorfmüller are grateful to the 'Stiftung Volkswagenwerk' for financial support. The allocation of CPU time on the Convex C240 computer by the Rechenzentrum der Universität Bielefeld is acknowledged. The financial support of the 'Fonds der chemischen Industrie' is also acknowledged.

References

[1] SAMIOS, J., STASSEN, H and DORFMÜLLER, TH., 1991, *Chem. Phys.*, **160,** 33.
[2] DEAKIN, A. A. and WALMSLEY, S. H., 1989, *Chem. Phys.*, **136,** 105.
[3] GRAY, C. G. and GUBBINS, K. E., 1984, *Theory of Molecular Fluids, Volume 1: Fundamentals* (Clarendon Press) pp. 45–91.
[4] ALLEN, M. P. and TILDESLEY, D. J., 1987, *Computer Simulation of Liquids* (Clarendon Press) pp. 332–334.
[5] AMOS, R. D. and BATTAGLIA, M. R., 1978, *Molec. Phys.*, **36,** 1517.
[6] ZANDLER, M. E., WATSON JR., J. A. and EYRING, H., 1968, *J. Phys. Chem.*, **72,** 2730.
[7] MURRELL, J. N. and GUO, H., 1987, *Faraday Trans. II*, **83,** 683.
[8] FOORD, A., SMITH, J. G. and WHIFFEN, D. H., 1975, *Molec. Phys.*, **29,** 1685.
[9] SINGER, K., TAYLOR, A. and SINGER, J. V. L., 1977, *Molec. Phys.*, **33,** 1757.
[10] TILDESLEY, D. J. and MADDEN, P. A., 1983, *Molec. Phys.*, **48,** 129.
[11] SINGER, K., SINGER, J. V. L. and TAYLOR, A. J., 1979, *Molec. Phys.*, **37,** 1239.
[12] TILDESLEY, D. J. and MADDEN, P. A., 1981, *Molec. Phys.*, **42,** 1137.
[13] MURTHY, J. S., SINGER, K. and MCDONALD, I. R ., 1981, *Molec. Phys.*, **44,** 135.
[14] STONE, A. J. and ALDERTON, M., 1985, *Molec. Phys.*, **56,** 1047.